COMPUTATIONAL MATHEMATICS
ВЫЧИСЛИТЕЛЬНАЯ МАТЕМАТИКА

UDC 519.6

Original Theoretical Research

https://doi.org/10.23947/2587-8999-2025-9-2-22-33

Comparison of Solutions to a Hydrodynamic Problem in a Rectangular Cavity Using Initial Velocity Field Damping and Acceleration Methods

Natalya K. Volosova[1], Konstantin A. Volosov[2], Aleksandra K. Volosova[2], Mikhail I. Karlov[3], Dmitriy F. Pastukhov[4] ✉, Yuriy F. Pastukhov[4]

[1] MGTU named after. N.E. Bauman, Moscow, Russian Federation

[2] Russian University of Transport, Moscow, Russian Federation

[3] Moscow Institute of Physics and Technology (National Research University), Dolgoprudny, Russian Federation

[4] Polotsk State University named after Euphrosyne of Polotsk, Novopolotsk, Republic of Belarus

✉ dmitrij.pastuhov@mail.ru

Abstract

Introduction. This study investigates the numerical solution of a two-dimensional hydrodynamic problem in a rectangular cavity using the method of initial velocity field damping and the method of accelerating the initial conditions in terms of stream function and vorticity variables. The damping method was applied at Reynolds numbers Re ≤ 3000, and the acceleration method was used for Re = 8000.

Materials and Methods. To speed up the numerical solution of the problem using an explicit finite-difference scheme for the vorticity dynamics equation, the method of initial condition damping and the method of *n*-fold splitting of the explicit difference scheme (with $n = 100$) were used. Compared to the traditional method of accelerating from stationary fluid, the initial velocity field damping method reduced the computation time by a factor of 57. The splitting method used a maximum time step proportional to the square of the spatial step, while maintaining spectral stability of the explicit scheme in the vorticity equation. The majority of computation time was spent solving the Poisson equation in the "stream function — vorticity" variables. By freezing the velocity field and solving only the vorticity dynamics equation, computation time was further reduced in the splitting method. The inverse matrix for solving the Poisson equation using a finite number of elementary operations were computed using the Msimsl library.

Results. Numerical solutions demonstrated the equivalence of the damping and acceleration methods for the initial velocity field at low Reynolds numbers (up to 3000). The equivalence of solutions obtained using the "stream function — vorticity" algorithm and the implicit iterated polyneutic recurrent method for accelerated initial conditions was numerically confirmed. For the first time, an initial horizontal velocity field was proposed, smooth at internal points and composed of two sine waves, with a stationary center of mass for the fluid in the rectangular cavity.

Discussion and Conclusion. An algorithm for numerically solving a two-dimensional hydrodynamic problem in a rectangular cavity using "stream function — vorticity" variables is proposed. The approximation of the equations in system (1) has sixth-order accuracy at internal grid points and fourth-order accuracy at boundary points. A novel damping method is introduced using an initial horizontal velocity field formed by smoothly connecting two sine waves. The proposed algorithms enhance the efficiency of solving hydrodynamic problems using an explicit finite-difference scheme for the vorticity equation.

Keywords: hydrodynamics, numerical methods, partial differential equations, initial-boundary value problem, boundary conditions, initial conditions

For Citation. Volosova N.K., Volosov K.A., Volosova A.K., Karlov M.I., Pastukhov D.F., Pastukhov Yu.F. Comparison of Solutions to a Hydrodynamic Problem in a Rectangular Cavity Using Initial Velocity Field Damping and Acceleration Methods. *Computation Mathematics and Information Technologies*. 2025;9(2):22–33. https://doi.org/10.23947/2587-8999-2025-9-2-22-33

Оригинальное теоретическое исследование

Сравнение решений гидродинамической задачи в прямоугольной каверне методами торможения и разгона начального поля скорости

Н.К. Волосова[1], К.А. Волосов[2], А.К. Волосова[2], М.И. Карлов[3], Д.Ф. Пастухов[4] ✉, Ю.Ф. Пастухов[4]

[1] Московский государственный технический университет им. Н.Э. Баумана, г. Москва, Российская Федерация

[2] Российский университет транспорта, г. Москва, Российская Федерация

[3] Московский физико-технический институт (национальный исследовательский университет), г. Долгопрудный, Российская Федерация

[4] Полоцкий государственный университет им. Евфросинии Полоцкой, г. Новополоцк, Республика Беларусь

✉ dmitrij.pastuhov@mail.ru

Аннотация

Введение. Исследуется численное решение двумерной гидродинамической задачи в прямоугольной каверне методом торможения и методом разгона начальных условий в переменных «функция тока — вихрь». Метод торможения применялся при числах Рейнольдса $Re \le 3000$, а метод разгона при числах $Re = 8000$.

Материалы и методы. Для ускорения численного решения задачи с явной разностной схемой уравнения динамики вихря использовался метод торможения начальных условий и метод n-кратного расщепления явной разностной схемы ($n = 100$). Метод торможения начальных условий поля скорости по сравнению с методом разгона неподвижной жидкости позволил сократить время счета задачи в 57 раз. Метод расщепления использовал максимальный шаг времени, пропорциональный квадрату координатного шага, не нарушая при этом спектральной устойчивости явной схемы в уравнении вихря. Наибольшее время программа затратила на решение уравнения Пуассона с переменными «функция тока — вихрь». Используя замороженное поле скоростей и решая только динамическое уравнение вихря, было сокращено время счета в методе расщепления. Обратная матрица для решения уравнения Пуассона за конечное число элементарных операций вычислялась библиотекой Msimsl.

Результаты исследования. Численное решение задачи показало эквивалентность методов торможения и разгона начального поля скорости при небольших числах Рейнольдса (до 3000). Численно доказана эквивалентность решения гидродинамической задачи алгоритмом в переменных «функция тока — вихрь» и алгоритмом с неявным полилинейным рекуррентным методом в случае разгона начальных условий. Впервые предложено начальное горизонтальное поле скорости, гладкое во внутренних точках и состоящее из двух синусоид с неподвижным центром масс всей жидкости в прямоугольной каверне.

Обсуждение и заключение. Предложен алгоритм численного решения двухмерной гидродинамической задачи в прямоугольной каверне в переменных «функция тока — вихрь». Аппроксимация уравнений в системе (1) имеет шестой порядок погрешности во внутренних узлах и четвертый в граничных узлах. Впервые предложен метод торможения с начальным полем горизонтальной скорости посредством гладкого соединения двух синусоид. Предложенные алгоритмы позволяют более эффективно решать задачи гидродинамики с явной разностной схемой уравнения вихря.

Ключевые слова: гидродинамика, численные методы, уравнения в частных производных, начально-краевая задача, граничные условия, начальные условия

Для цитирования. Волосова Н.К., Волосов К.А., Волосова А.К., Карлов М.И., Пастухов Д.Ф., Пастухов Ю.Ф. Сравнение решений гидродинамической задачи в прямоугольной каверне методами торможения и разгона начального поля скорости. *Computational Mathematics and Information Technologies*. 2025;9(2):22–33. https://doi.org/10.23947/2587-8999-2025-9-2-22-33

Introduction. This paper examines a two-dimensional hydrodynamic problem in a rectangular cavity with a moving upper lid, formulated in the “stream function — vorticity” variables [1]. The velocity field features two singular points in the upper corners of the cavity—both in magnitude and direction—making this problem a benchmark for testing numerical algorithms designed to solve various hydrodynamic problems [2]. For instance, studies [3–5] focus on exact or highly accurate approximate solutions to hydrodynamic problems. Problems involving large velocity field gradients at singular points are presented in [6, 7], while flows in viscous fluids are addressed in [8, 9]. Several approaches to formulating initial and boundary conditions in hydrodynamics are discussed in [10, 11].

The present work builds upon the method of n-fold splitting of the vorticity equation using an explicit finite-difference scheme ($n = 100$), as described in [11], and employs a uniform grid $n_1 \times n_2 = 100 \times 100$.

Materials and Methods

Problem Statement. We consider the classical hydrodynamic problem in a rectangular domain (cavity), described by a system of partial differential equations along with initial and boundary conditions for the physical fields [1], formulated

in the "stream function — vorticity" variables. Let ($u(x,y)$, $v(x,y)$) denote the velocity vector of a fluid particle. On the solid boundaries — the lateral and bottom sides of the rectangular cavity — the velocity is zero (no-slip condition for fluid particles). The normal component of the velocity is also zero along the entire rectangular boundary. We position the origin of the coordinate system at the lower left corner of the rectangle, with the y-axis directed upward and the x-axis to the right. Let L be the width of the rectangular cavity and H its height.

In this hydrodynamic problem within a closed cavity, the moving upper lid translates to the right with a constant velocity $u_{\max}$. We define the characteristic scales: length scale: L, time scale: $\frac{L}{u_{\max}}$, velocity scale: $u_{\max}$, stream function scale: $Lu_{\max}$, vorticity scale: $\frac{u_{\max}}{L}$, Reynolds number: Re. We introduce the following dimensionless variables: $\bar{x}$ is the horizontal coordinate, $\bar{y}$ is the vertical coordinate, $\bar{\psi}$, $\bar{w}$ are the stream function and vorticity, respectively, $(\bar{u}, \bar{v})$ is the dimensionless velocity vector, $\bar{t}$ is the dimensionless time:

$$0 \le \bar{x} = \frac{x}{L} \le 1,\ 0 \le \bar{y} = \frac{y}{L} \le k = \frac{H}{L}, \bar{\psi} = \frac{\psi}{\psi_{\max}}, \psi_{\max} = Lu_{\max},$$

$$\bar{u} = \frac{u}{u_{\max}}, \bar{v} = \frac{v}{u_{\max}} \bar{w} = \frac{w}{w_{\max}}, w_{\max} = \frac{u_{\max}}{L},$$

$$\bar{t} = \frac{t}{T}, T = \frac{L}{u_{\max}}, \mathrm{Re} = \frac{u_{\max} L}{\nu}.$$

Let us write the system of hydrodynamic equations using the dimensionless variables and functions [1, 5, 11]:

$$\begin{cases} \bar{\psi}_{\bar{x}\bar{x}} + \bar{\psi}_{\bar{y}\bar{y}} = -\bar{w}(\bar{x}, \bar{y}),\ 0 < \bar{x} = \frac{x}{L} < 1,\ 0 < \bar{y} < k_{\max}, \\ \bar{w} = \bar{v}_{\bar{x}} - \bar{u}_{\bar{y}}, \\ \bar{u} = \bar{\psi}_{\bar{y}}; \bar{v} = -\bar{\psi}_{\bar{x}}, \\ \bar{w}_{\bar{t}} + \bar{u} \cdot \bar{w}_{\bar{x}} + \bar{v} \cdot \bar{w}_{\bar{y}} = \frac{1}{\mathrm{Re}} \left(\bar{w}_{\bar{x}\bar{x}} + \bar{w}_{\bar{y}\bar{y}} \right), 0 < \bar{t} = \frac{t}{T}, \\ \bar{\psi}\big|_{\Gamma} \equiv 0, \bar{v}\big|_{\Gamma} \equiv 0, \bar{u}\big|_{\Gamma_1} = 0, \bar{u}\big|_{\Gamma \setminus \Gamma_1} = 1. \end{cases} \tag{1}$$

Here Γ_1 denotes the union of the side walls and the bottom segment of the rectangular boundary, $\Gamma \setminus \Gamma_1$ represents the upper segment of the rectangle. The first equation in system (1) is the Poisson equation for the stream function and vorticity. The two-dimensional Poisson equation on a rectangular domain is solved in matrix form using a finite number of arithmetic operations with sixth-order accuracy [5, 12]. From this point forward, we will omit the overbars above the dimensionless functions, time, and coordinates for convenience.

The second line of system (1) describes the vorticity function, which is computed through the spatial derivatives of the velocity field. The third line calculates the velocity components as partial derivatives of the stream function. The fourth line is the vorticity dynamics equation, the only one in system (1) that explicitly depends on time. On the left-hand side is the total (convective) time derivative. On the boundary of the rectangle, the vertical component of velocity is zero; the horizontal component is equal to one on the upper segment and zero on the bottom and side segments.

In addition to the two mentioned singular points of the velocity field, for testing the algorithm in the method of initial velocity field damping, a highly unsteady and vortical initial velocity field was used. This field should, by its parameters, be close to a steady-state velocity field, satisfy the continuity equation for incompressible flow, and—as numerical experiments show—be continuously differentiable at all points in the domain.

For the first time in this work, an initial horizontal velocity field on a uniform rectangular grid is proposed, defined by formula (2). The horizontal velocity profile on the upper segment of the rectangular cavity is constructed by smoothly stitching together two cubic polynomials:

$$u(x_n, y_m) = \begin{cases} u_-(x_n, y_m) = -\frac{u_0(x_n)}{\sqrt{2}} \sin\left(\frac{\pi y_m}{k_1} \right) = -\frac{u_0(x_n)}{\sqrt{2}} \sin\left(\frac{\left(1+\sqrt{2}\right)\pi y_m}{k\sqrt{2}} \right), 0 \le y_m \le \frac{\sqrt{2}}{1+\sqrt{2}} k, \\ u_+(x_n, y_m) = u_0(x_n) \sin\left(\frac{\pi(y_m - k_1)}{2k_2} \right) = u_0(x_n) \sin\left(\frac{\pi}{2} \frac{\left(y_m - \frac{\sqrt{2}k}{1+\sqrt{2}} \right)}{\frac{k}{1+\sqrt{2}}} \right), \frac{\sqrt{2}}{1+\sqrt{2}} k < y_m \le k, \\ x_n = nh_1, y_m = mh_2, h_1 = \frac{1}{n_1}, h_2 = \frac{k}{n_2}, k_1 = \frac{\sqrt{2}k}{1+\sqrt{2}}, k_2 = \frac{k}{1+\sqrt{2}}, k_1 + k_2 = k, k_1 = \sqrt{2}k_2, \\ n = \overline{0, n_1}, m = \overline{0, n_2}, n_1 = n_2 = 100. \end{cases} \tag{2}$$

In formula (2), the lower part of the fluid moves to the left, the upper part moves to the right, and the horizontal component of the velocity is bounded by $u_0(x_n)$, i. e., it does not exceed unity. The profile of the horizontal velocity is continuous with respect to the variable y: $u_-(x_n,0)=u_-(x_n,k_1)=u_+(x_n,k_1)=0, u_+(x_n,k)=u_0(x_n)$. At the boundary point, the sine curve graphs are tangent to each other:

$$u_{-y}(x_n,k_1)=u_{+y}(x_n,k_1)\Leftrightarrow -\frac{u_0(x_n)}{\sqrt{2}}\frac{\pi}{k_1}\cos\left(\frac{\pi k_1}{k_1}\right)=\frac{u_0(x_n)}{\sqrt{2}}\frac{\pi}{k_1}=u_0(x_n)\frac{\pi}{2k_2}\cos\left(\frac{\pi(k_1-k_1)}{2k_2}\right)=u_0(x_n)\frac{\pi}{2k_2}=u_0(x_n)\frac{\pi}{\sqrt{2}k_1}.$$

Integrating the profile (2) with respect to y from 0 to k while keeping the variable x, constant, and denoting the integral by $\overline{y}\Big|_0^1=\frac{y\big|_0^{k_1}}{k_1}, \overline{\overline{y}}\Big|_0^1=\frac{(y-k_1)\big|_{k_1}^{k=k_1+k_2}}{k_2}$ we get:

$$\int_0^k u(x,y)dy=\int_0^{k_1}u_-(x,y)dy+\int_{k_1}^{k_1+k_2}u_+(x,y)dy=u_0(x)\left(-\frac{k_1}{\sqrt{2}}\int_0^1\sin(\pi\overline{y})d\overline{y}+k_2\int_0^1\sin\left(\frac{\pi}{2}\overline{\overline{y}}\right)d\overline{\overline{y}}\right)=$$

$$=u_0(x)\left(\frac{k_1}{\sqrt{2}\pi}\cos(\pi\overline{y})\Big|_0^1-\frac{2k_2}{\pi}\cos\left(\frac{\pi}{2}\overline{\overline{y}}\right)\Big|_0^1\right)=u_0(x)\left(\frac{-2k_1}{\sqrt{2}\pi}+\frac{2k_2}{\pi}\right)=u_0(x)\left(\frac{-\sqrt{2}k_1}{\pi}+\frac{\sqrt{2}k_1}{\pi}\right)=0.$$

This last integral shows that, at the initial moment in time, the center of mass of each sufficiently thin vertical column of fluid lies on the x-axis. Thus, according to the law of conservation of momentum, the center of mass of the entire fluid does not move along the x-axis either initially or at any subsequent moment in time.

The profile of the horizontal velocity component (3) on the upper segment of the cavity ($y = k = 1$) had the form of a smooth and continuous symmetric curved trapezoid without singular points in the velocity field:

$$u(x,k)\equiv u_0(x)=\begin{cases}3z^2\text{-}2z^3, z=\dfrac{x}{\tau}\in[0,1], 0\le x\le\tau, \tau=\dfrac{n_0}{n_1}=\dfrac{1}{10},\\ 1, \tau\le x\le 1-\tau,\\ 3z^2\text{-}2z^3, z=\dfrac{1-x}{\tau}\in[0,1], 1-\tau\le x\le 1.\end{cases} \tag{3}$$

Note that $u(0)=u'(0)=\left(6z-6z^2\right)_{z=0}=0, u(1)=1, u'(1)=\left(6z-6z^2\right)_{z=1}=0$, i. e., at the two junction points $x=\tau$, $x = 1 - \tau$ the profile of the horizontal component of velocity on the upper segment of the rectangular cavity is smooth.

The vertical component of the fluid particle velocity at the initial moment, according to the continuity equation, was calculated using the trapezoidal rule $m=\overline{1,n_2-1}, n=\overline{1,n_1-1}$:

$$v(x_n,y_m)=-h_2\left(\frac{u_x(x_n,y_m)}{2}+\sum_{i=1}^{m-1}u_x(x_n,y_i)\right)=-h_2\left(\frac{u(x_{n+1},y_m)-u(x_{n-1},y_m)}{4h_1}+\sum_{i=1}^{m-1}\frac{u(x_{n+1},y_i)-u(x_{n-1},y_i)}{2h_1}\right). \tag{4}$$

According to the algorithm described in [1], the first equation to be solved in system (1) is the Poisson equation, which is computed using a finite number of elementary operations [5]. The Poisson equation is approximated with sixth-order accuracy at all internal points.

To approximate the Laplace operator, we expand the nodal values of the stream function $\psi(x, y)$ in a Taylor series around the central node on a 3×3 rectangular stencil. Due to symmetry, the odd-order partial derivatives of the stream function vanish. When expanding in a Taylor series, we also take into account the Poisson equation:

$$\Delta\psi=\psi_{xx}+\psi_{yy}=f(x,y)=-w\Leftrightarrow\psi_{xx}\big|_{(x_i,y_j)}+\psi_{yy}\big|_{(x_i,y_j)}=f(x_i,y_j)=f_{i,j}, i=\overline{1,n_2-1}, j=\overline{1,n_1-1}, \tag{5}$$

$$\Delta\psi=\frac{1}{h^2}\left(C_0\psi_{0,0}+C_1\left(\psi_{-1,0}+\psi_{0,-1}+\psi_{1,0}+\psi_{0,1}\right)+C_2\left(\psi_{-1,-1}+\psi_{1,-1}+\psi_{-1,1}+\psi_{1,1}\right)\right)=\frac{1}{h^2}\left(\psi_{0,0}\left(C_0+4C_1+4C_2\right)+\right.$$

$$+C_1\left(h^2\left(\psi_{xx}+\psi_{yy}\right)+\frac{h^4}{12}\left(\psi_x^{(4)}+\psi_y^{(4)}\right)+\frac{h^6}{360}\left(\psi_x^{(6)}+\psi_y^{(6)}\right)+O\left(h^8\right)\right)+$$

$$+C_2\left(2h^2\left(\psi_{xx}+\psi_{yy}\right)+\frac{h^4}{6}\left(\psi_x^{(4)}+\psi_y^{(4)}+6\psi_{xxyy}^{(4)}\right)+\frac{h^6}{180}\left(\psi_x^{(6)}+\psi_y^{(6)}+15\left(\psi_{xxxxyy}^{(6)}+\psi_{xxyyyy}^{(6)}\right)\right)+O\left(h^8\right)\right)= \tag{6}$$

$$=\frac{\psi_{0,0}\left(C_0+4C_1+4C_2\right)}{h^2}+\left(C_1+2C_2\right)\left(\psi_{xx}+\psi_{yy}\right)+\frac{h^2}{12}\left(\left(\psi_x^{(4)}+\psi_y^{(4)}\right)C_1+2C_2\left(\psi_x^{(4)}+\psi_y^{(4)}+6\psi_{xxyy}^{(4)}\right)\right)+$$

$$+h^4\left(\left(\psi_x^{(6)}+\psi_y^{(6)}\right)\frac{C_1}{360}+\left(\psi_x^{(6)}+\psi_y^{(6)}+15\left(\psi_{xxxxyy}^{(6)}+\psi_{xxyyyy}^{(6)}\right)\right)\frac{C_2}{180}\right)+O\left(h^6\right)=\Delta\psi=\psi_{xx}+\psi_{yy}.$$

Using equation (5) for equation (6), as well as the boundedness of the solution at each node of the rectangular grid, we get that

$$\begin{cases} C_0 + 4C_1 + 4C_2 = 0, \\ C_1 + 2C_2 = 1. \end{cases}$$

Note that

$$\Delta f = \Delta\left(\psi_{xx} + \psi_{yy}\right) = \left(\frac{\partial^2}{\partial x^2} + \frac{\partial^2}{\partial y^2}\right)\left(\psi_{xx} + \psi_{yy}\right) = \psi_x^{(4)} + \psi_y^{(4)} + 2\psi_{xxyy}^{(4)} = f_{xx} + f_{yy},$$

$$\Delta^2 f = \Delta\left(\psi_x^{(4)} + \psi_y^{(4)} + 2\psi_{xxyy}^{(4)}\right) = \psi_x^{(6)} + \psi_y^{(6)} + 3\left(\psi_{xxxxyy}^{(6)} + \psi_{xxyyyy}^{(6)}\right), f_{xxyy}^{(4)} = \left(\psi_{xx} + \psi_{yy}\right)_{xxyy} = \psi_{xxyyyy}^{(6)} + \psi_{yyxxxx}^{(6)}.$$

Considering the transformations above, we can rewrite formula (6) as:

$$\Delta\psi = \psi_{xx} + \psi_{yy} + \frac{h^2}{12}\left(\left(\psi_x^{(4)} + \psi_y^{(4)}\right)\left(C_1 + 2C_2\right) + 12C_2\psi_{xxyy}^{(4)}\right) +$$
$$+h^4\left(\left(\psi_x^{(6)} + \psi_y^{(6)}\right)\frac{C_1}{360} + \left(\psi_x^{(6)} + \psi_y^{(6)} + 15\left(\psi_{xxxxyy}^{(6)} + \psi_{xxyyyy}^{(6)}\right)\right)\frac{C_2}{180}\right) + O\left(h^6\right).$$

We require that the coefficient of $\frac{h^2}{12}$ becomes an operator Δf acting on the function f. Therefore, we have:

$$12C_2 = 2,$$

$$\begin{cases} C_0 + 4C_1 + 4C_2 = 0 \\ C_1 + 2C_2 = 1 \\ 12C_2 = 2 \end{cases} \Leftrightarrow C_2 = \frac{1}{6}, C_1 = 1 - 2C_2 = \frac{2}{3}, C_0 = -4C_1 - 4C_2 = -\frac{10}{3},$$

$$\begin{aligned} &\Delta\psi = f + \frac{h^2}{12}\Delta f + \frac{h^4}{360}\left(C_1 + 2C_2\right)\left(\psi_x^{(6)} + \psi_y^{(6)}\right) + \frac{h^4\left(\psi_{xxxxyy}^{(6)} + \psi_{xxyyyy}^{(6)}\right)}{72} + O\left(h^6\right) \Leftrightarrow \\ &\Leftrightarrow \frac{1}{h^2}\left(-\frac{10}{3}\psi_{0,0} + \frac{2}{3}\left(\psi_{-1,0} + \psi_{0,-1} + \psi_{1,0} + \psi_{0,1}\right) + \frac{1}{6}\left(\psi_{-1,-1} + \psi_{1,-1} + \psi_{-1,1} + \psi_{1,1}\right)\right) = \\ &= f + \frac{h^2}{12}\Delta f + \frac{h^4}{360}\left(\psi_x^{(6)} + \psi_y^{(6)} + 3\left(\psi_{xxxxyy}^{(6)} + \psi_{xxyyyy}^{(6)}\right)\right) + \left(\psi_{xxxxyy}^{(6)} + \psi_{xxyyyy}^{(6)}\right)\left(\frac{5}{360} - \frac{1}{120}\right) + O\left(h^6\right) = \\ &= f + \frac{h^2}{12}\Delta f + \frac{h^4}{360}\Delta^2 f + \frac{h^4 f_{xxyy}^{(4)}}{180} + O\left(h^6\right) = f + \frac{h^2}{12}\left(f_{xx} + f_{yy}\right) + \frac{h^4}{360}\left(f_x^{(4)} + f_y^{(4)}\right) + \frac{h^4 f_{xxyy}^{(4)}}{90} + O\left(h^6\right). \end{aligned} \tag{7}$$

To use the Poisson equation (7) for the stream function in the system of equations (1) with an accuracy of $O(h^6)$ it is necessary $f = -w$, the derivatives f_{xx}, f_{yy} be represented with an accuracy of $O(h^4)$, and $f_x^{(4)}, f_y^{(4)}, f_{xxyy}^{(4)}$ with an accuracy of $O(h^2)$.

Using the method of undetermined coefficients [12], formulas for the internal nodes of the function f with indices $n = \overline{2, n_1 - 2}, m = \overline{2, n_2 - 2}$ were obtained:

$$\begin{cases} f_{xx} + f_{yy} = \frac{1}{h^2}\left(-5f_{0,0} + \frac{4}{3}\left(f_{-1,0} + f_{0,-1} + f_{1,0} + f_{0,1}\right) - \frac{1}{12}\left(f_{-2,0} + f_{0,-2} + f_{2,0} + f_{0,2}\right)\right) + O\left(h^4\right), \\ f_x^{(4)} + f_y^{(4)} = \frac{1}{h^4}\left(12f_{0,0} - 4\left(f_{-1,0} + f_{0,-1} + f_{1,0} + f_{0,1}\right) + f_{-2,0} + f_{0,-2} + f_{2,0} + f_{0,2}\right) + O\left(h^2\right), \\ f_{xxyy}^{(4)} = \frac{1}{h^4}\left(4f_{0,0} - 2\left(f_{-1,0} + f_{0,-1} + f_{1,0} + f_{0,1}\right) + f_{-1,-1} + f_{-1,1} + f_{1,-1} + f_{1,1}\right) + O\left(h^2\right). \end{cases} \tag{8}$$

Thus, formulas (7) and (8) together approximate the Poisson equation for the stream function and the vorticity function in (1) with sixth-order accuracy at the interior nodes of the rectangle.

In [5], an algorithm for the matrix method of solving the difference Poisson equation (7) is described, which involves a finite number of elementary arithmetic operations using the vector sweep method.

Consider the difference equation (9):

$$\begin{aligned} &\frac{1}{h^2}\left(\frac{-10}{3}\psi_{m,n} + \frac{2}{3}\left(\psi_{m-1,n} + \psi_{m+1,n} + \psi_{m,n-1} + \psi_{m,n+1}\right) + \frac{1}{6}\left(\psi_{m-1,n-1} + \psi_{m+1,n-1} + \psi_{m-1,n+1} + \psi_{m+1,n+1}\right)\right) = f_{m,n} + \frac{h^2}{12}\left(f_{xx} + f_{yy}\right) + \\ &+h^4\left(\frac{1}{360}\left(f_x^{(4)} + f_y^{(4)}\right) + \frac{1}{90}f_{xxyy}^{(4)}\right) + O\left(h^6\right) \equiv F_{m,n}, \quad n = \overline{1, n_1 - 1}, m = \overline{1, n_2 - 1}. \end{aligned} \tag{9}$$

We define square matrices A, B of dimension $(n_1-1)\times(n_1-1)$:

$$a_{m,n}=\begin{cases}-\frac{10}{3}, m=n; m=\overline{1,n_1-1}, n=\overline{1,n_1-1},\\ \frac{2}{3}, m=n+1\vee m=n-1,\\ 0, m\ge n+2\vee m\le n-2,\end{cases}\qquad b_{m,n}=\begin{cases}\frac{2}{3}, m=n; m=\overline{1,n_1-1}, n=\overline{1,n_1-1},\\ \frac{1}{6}, m=n+1\vee m=n-1,\\ 0, m\ge n+2\vee m\le n-2.\end{cases} \tag{10}$$

Let us briefly write the matrix algorithm for solving the difference equation (9) [5]:

1. Using the formula:

$$F^T{}_{m,n}=f_{m,n}h^2+\frac{h^4}{12}\left(f_{xx}+f_{yy}\right)+h^6\left(\frac{1}{360}\left(f_x^{(4)}+f_y^{(4)}\right)+\frac{1}{90}f_{xxyy}^{(4)}\right)+O\left(h^8\right)\Big|_{x=x_n,y=y_m}$$

compute the right-hand side of the Poisson equation at all interior nodes of the uniform grid of the rectangle (m = 1, …, n_2 – 1; n = 1, …, n_1 – 1).

2. Modify the right-hand side of the system of equations (11) using formulas (12) and (13) at the nodes of the rectangular contour adjacent to the boundary contour, i. e., calculate $\overline{F_{m,n}}$ based on the values $F_{m,n}$ from step 1:

$$\begin{cases}A\psi_1^T+B\psi_2^T=\overline{F_1^T},\\ B\psi_{m-1}^T+A\psi_m^T+B\psi_{m+1}^T=\overline{F_m^T}, m=\overline{2,n_2-2},\\ B\psi_{n_2-2}^T+A\psi_{n_2-1}^T=\overline{F_{n_2-1}^T}.\end{cases} \tag{11}$$

$$\begin{cases}\frac{-10}{3}\psi_{1,n_1-1}+\frac{2}{3}\left(\psi_{2,n_1-1}+\psi_{1,n_1-2}+\psi_{1,n_1}+\psi_{0,n_1-1}\right)+\frac{1}{6}\left(\psi_{2,n_1-2}+\psi_{0,n_1-2}+\psi_{2,n_1}+\psi_{0,n_1}\right)=F_{1,n_1-1},\\ \overline{F_{1,n_1-1}}\equiv F_{1,n_1-1}-\frac{2}{3}\left(\psi_{1,n_1}+\psi_{0,n_1-1}\right)-\frac{1}{6}\left(\psi_{0,n_1-2}+\psi_{2,n_1}+\psi_{0,n_1}\right),\\ \frac{-10}{3}\psi_{n_2-1,1}+\frac{2}{3}\left(\psi_{n_2-2,1}+\psi_{n_2-1,2}+\psi_{n_2-1,0}+\psi_{n_2,1}\right)+\frac{1}{6}\left(\psi_{n_2-2,2}+\psi_{n_2,2}+\psi_{n_2-2,0}+\psi_{n_2,0}\right)=F_{n_2-1,1},\\ \overline{F_{n_2-1,1}}\equiv F_{n_2-1,1}-\frac{2}{3}\left(\psi_{n_2-1,0}+\psi_{n_2,1}\right)-\frac{1}{6}\left(\psi_{n_2,2}+\psi_{n_2-2,0}+\psi_{n_2,0}\right),\\ \frac{-10}{3}\psi_{n_2-1,n_1-1}+\frac{2}{3}\left(\psi_{n_2-2,n_1-1}+\psi_{n_2-1,n_1-2}+\psi_{n_2-1,n_1}+\psi_{n_2,n_1-1}\right)+\frac{1}{6}\left(\psi_{n_2-2,n_1-2}+\psi_{n_2,n_1-2}+\psi_{n_2-2,n_1}+\psi_{n_2,n_1}\right)=F_{n_2-1,n_1-1},\\ \overline{F_{n_2-1,n_1-1}}\equiv F_{n_2-1,n_1-1}-\frac{2}{3}\left(\psi_{n_2-1,n_1}+\psi_{n_2,n_1-1}\right)-\frac{1}{6}\left(\psi_{n_2,n_1-2}+\psi_{n_2-2,n_1}+\psi_{n_2,n_1}\right),\\ \frac{-10}{3}\psi_{1,1}+\frac{2}{3}\left(\psi_{2,1}+\psi_{1,2}+\psi_{1,0}+\psi_{0,1}\right)+\frac{1}{6}\left(\psi_{2,2}+\psi_{0,2}+\psi_{2,0}+\psi_{0,0}\right)=F_{1,1},\\ \overline{F_{1,1}}\equiv F_{1,1}-\frac{2}{3}\left(\psi_{1,0}+\psi_{0,1}\right)-\frac{1}{6}\left(\psi_{0,2}+\psi_{2,0}+\psi_{0,0}\right).\end{cases} \tag{12}$$

$$\begin{cases}-\frac{10}{3}\psi_{1,n}+\frac{2}{3}\left(\psi_{1,n-1}+\psi_{2,n}+\psi_{1,n+1}+\psi_{0,n}\right)+\frac{1}{6}\left(\psi_{2,n-1}+\psi_{2,n+1}+\psi_{0,n-1}+\psi_{0,n+1}\right)=F_{1,n}, n=\overline{2,n_1-2},\\ \overline{F_{1,n}}=F_{1,n}-\frac{2}{3}\psi_{0,n}-\frac{1}{6}\left(\psi_{0,n-1}+\psi_{0,n+1}\right), n=\overline{2,n_1-2},\\ -\frac{10}{3}\psi_{n_2-1,n}+\frac{2}{3}\left(\psi_{n_2-1,n-1}+\psi_{n_2-2,n}+\psi_{n_2-1,n+1}+\psi_{n_2,n}\right)+\frac{1}{6}\left(\psi_{n_2-2,n-1}+\psi_{n_2-2,n+1}+\psi_{n_2,n-1}+\psi_{n_2,n+1}\right)=F_{n_2-1,n}, n=\overline{2,n_1-2},\\ \overline{F_{n_2-1,n}}=F_{n_2-1,n}-\frac{2}{3}\psi_{n_2,n}-\frac{1}{6}\left(\psi_{n_2,n-1}+\psi_{n_2,n+1}\right), n=\overline{2,n_1-2},\\ -\frac{10}{3}\psi_{m,1}+\frac{2}{3}\left(\psi_{m-1,1}+\psi_{m,2}+\psi_{m+1,1}+\psi_{m,0}\right)+\frac{1}{6}\left(\psi_{m-1,2}+\psi_{m+1,2}+\psi_{m-1,0}+\psi_{m+1,0}\right)=F_{m,1}, m=\overline{2,n_2-2},\\ \overline{F_{m,1}}=F_{m,1}-\frac{2}{3}\psi_{m,0}-\frac{1}{6}\left(\psi_{m-1,0}+\psi_{m+1,0}\right), m=\overline{2,n_2-2},\\ -\frac{10}{3}\psi_{m,n_1-1}+\frac{2}{3}\left(\psi_{m-1,n_1-1}+\psi_{m,n_1-2}+\psi_{m+1,n_1-1}+\psi_{m,n_1}\right)+\frac{1}{6}\left(\psi_{m-1,n_1-2}+\psi_{m+1,n_1-2}+\psi_{m-1,n_1}+\psi_{m+1,n_1}\right)=F_{m,n_1-1}, m=\overline{2,n_2-2},\\ \overline{F_{m,n_1-1}}=F_{m,n_1-1}-\frac{2}{3}\psi_{m,n_1}-\frac{1}{6}\left(\psi_{m-1,n_1}+\psi_{m+1,n_1}\right), m=\overline{2,n_2-2},\\ \overline{F_{m,n}}=F_{m,n},\ \forall m\in\overline{2,n_2-2}, n\in\overline{2,n_1-2}.\end{cases} \tag{13}$$

3. Find the matrix coefficients for the forward sweep using formulas (14) and (15) $m = \overline{1, n_2 - 2}$:

$$\lambda_1 = -A^{-1}B, \nu_1 = A^{-1}\overline{F_1^T}, \tag{14}$$

$$\lambda_m = -\left(B\lambda_{m-1} + A\right)^{-1} B, \nu_m = \left(B\lambda_{m-1} + A\right)^{-1}\left(\overline{F_m^T} - B\nu_{m-1}\right), m = \overline{2, n_2 - 2}. \tag{15}$$

4. Find the vector-row $\psi^T_{n_2-1}$ using formula (16):

$$\psi^T_{n_2-1} = \left(B\lambda_{n_2-2} + A\right)^{-1}\left(\overline{F^T_{n_2-1}} - B\nu_{n_2-2}\right). \tag{16}$$

5. Find the remaining rows of the solution matrix ψ^T_m using formulas (17):

$$m = \overline{n_2 - 2, 1}\ \psi^T_m = \lambda_m \psi^T_{m+1} + \nu_m, m = \overline{n_2 - 2, 1}, \nu_{n_2-1} = \psi^T_{n_2-1}. \tag{17}$$

The matrix algorithm for the sweep (9)–(17) preserves sixth-order accuracy according to formulas (7) and (8) for the Poisson equation.

The second and third equations of the system (1) $\overline{w} = \overline{v}_{\overline{x}} - \overline{u}_{\overline{y}}, \overline{u} = \overline{\psi}_{\overline{y}}, \overline{v} = -\overline{\psi}_{\overline{x}}$ are linear with respect to the first partial derivatives, which can be calculated independently. Let us present the quadrature formulas for the first derivative with different stencil centers.

For example, for the equation $\overline{u} = \overline{\psi}_{\overline{y}}$ we obtain:

$$\begin{cases} u_{(i,j)} = \dfrac{1}{h}\left(\dfrac{3}{4}\left(\psi_{i+1,j} - \psi_{i-1,j}\right) - \dfrac{3}{20}\left(\psi_{i+2,j} - u_{i-2,j}\right) + \dfrac{1}{60}\left(\psi_{i+3,j} - \psi_{i-3,j}\right)\right) + O\left(h^6\right), i = \overline{3, n_2 - 3}, j = \overline{1, n_1 - 1}, \\ u_{(1,j)} = \dfrac{1}{h}\left(-\dfrac{\psi_{0,j}}{5} - \dfrac{13}{12}\psi_{1,j} + 2\psi_{2,j} - \psi_{3,j} + \dfrac{\psi_{4,j}}{3} - \dfrac{\psi_{5,j}}{20}\right) + O\left(h^4\right), j = \overline{1, n_1 - 1}, \\ u_{(2,j)} = \dfrac{1}{12h}\left(8\left(\psi_{3,j} - \psi_{1,j}\right) - \left(\psi_{4,j} - \psi_{0,j}\right)\right) + O\left(h^4\right), j = \overline{1, n_1 - 1}, \\ u_{(n_2-1,j)} = -\dfrac{1}{h}\left(-\dfrac{\psi_{n_2,j}}{5} - \dfrac{13}{12}\psi_{n_2-1,j} + 2\psi_{n_2-2,j} - \psi_{n_2-3,j} + \dfrac{\psi_{n_2-4,j}}{3} - \dfrac{\psi_{n_2-5,j}}{20}\right) + O\left(h^4\right), j = \overline{1, n_1 - 1}, \\ u_{(n_2-2,j)} = -\dfrac{1}{12h}\left(8\left(\psi_{n_2-3,j} - \psi_{n_2-1,j}\right) - \left(\psi_{n_2-4,j} - \psi_{n_2,j}\right)\right) + O\left(h^4\right), j = \overline{1, n_1 - 1}. \end{cases} \tag{18}$$

Similar formulas can be written for the equations $\overline{v} = -\overline{\psi}_{\overline{x}}, \overline{w} = \overline{v}_{\overline{x}} - \overline{u}_{\overline{y}}$. Consider the vortex dynamics equation in the system of equations (1). To accelerate the numerical solution of the problem (1), the splitting method [11] was used.

Analytically, the method of *n*-fold splitting of the vortex equation for the time interval $\tau_0 \cdot n$ can be written as:

$$\frac{w^{k+i+1} - w^{k+i}}{\tau_0} + u^k \cdot w_x^{k+i} + v^k \cdot w_y^{k+i} = \frac{1}{\mathrm{Re}}\left(w_{xx}^{k+i} + w_{yy}^{k+i}\right), i = \overline{0, n-1}. \tag{19}$$

The system of recurrence equations (19) for the vortex with a frozen velocity field $\left(u^k(x,y), v^k(x,y)\right), i = \overline{0, n-1}, k = const, k = 1,2,...$ consists of n intermediate steps $i = \overline{0, n-1}$, where the upper index *i* indicates the number of the intermediate time layer in the vortex equation (19), and the index k is the number of the multiple time layer in the system (19) (if *k* is a multiple of *n*). The velocity fields and stream functions are constant in equations (19) for given values of *k* = *const* and the change in index $i = \overline{0, n-1}$. In this system of equations, only the vortex field changes $w^{k+i}, i = \overline{0, n-1}$. The velocity field changes abruptly in systems (1) and (19) when the time index of the vortex function increases by *n* from *k* to *k* + *n* in the vortex equation system (19).

The idea of splitting the system of equations (19) is to reduce the accumulation of rounding errors and the computational time when solving it. Differential operators with respect to the coordinate in (19) are approximated in the internal nodes with accuracy $O(h^6)$, as are all the equations in the system (1), boundary conditions with accuracy $O(h^4)$, and the time with accuracy $O(\tau)$.

Thus, by solving equation (19) $\tau_0 \cdot n$, *n* times in time we get a time jump $\tau_0 \cdot n$ (which is *n* times larger than the sequential solution of the system of equations (1)) and reduce the rounding error without solving the other equations in the system (1) inside the system (19).

Equation (19) is linear with respect to the coordinate derivatives $w_x^i, w_y^i, w_{xx}^i, w_{yy}^i$. In work [11], it is shown that for spectral stability of the vortex dynamics equation (19), it is enough to choose the ratio of the time and spatial steps in the form of the inequality $\tau_0 \le \frac{3}{16}h^2\,\mathrm{Re}$. This maximum time step was set by the authors in the program.

For the first partial derivatives of equation (19), approximation formulas were used, for example, for w_y ((formulas for the derivative with respect to w_x are similar):

$$\begin{cases} w_{y(i,j)} = \frac{1}{h}\left(\frac{3}{4}\left(w_{i+1,j} - w_{i-1,j}\right) - \frac{3}{20}\left(w_{i+2,j} - w_{i-2,j}\right) + \frac{1}{60}\left(w_{i+3,j} - w_{i-3,j}\right)\right) + O\left(h^6\right), i = \overline{3, n_2 - 3}, j = \overline{1, n_1 - 1}, \\ w_{y(1,j)} = \frac{1}{h}\left(-\frac{w_{0,j}}{5} - \frac{13}{12}w_{1,j} + 2w_{2,j} - w_{3,j} + \frac{w_{4,j}}{3} - \frac{w_{5,j}}{20}\right) + O\left(h^4\right), j = \overline{1, n_1 - 1}, \\ w_{y(2,j)} = \frac{1}{12h}\left(8\left(w_{3,j} - w_{1,j}\right) - \left(w_{4,j} - w_{0,j}\right)\right) + O\left(h^4\right), j = \overline{1, n_1 - 1}, \\ w_{y(n_2-1,j)} = -\frac{1}{h}\left(-\frac{w_{n_2,j}}{5} - \frac{13}{12}w_{n_2-1,j} + 2w_{n_2-2,j} - w_{n_2-3,j} + \frac{w_{n_2-4,j}}{3} - \frac{w_{n_2-5,j}}{20}\right) + O\left(h^4\right), j = \overline{1, n_1 - 1}, \\ w_{y(n_2-2,j)} = -\frac{1}{12h}\left(8\left(w_{n_2-3,j} - w_{n_2-1,j}\right) - \left(w_{n_2-4,j} - w_{n_2,j}\right)\right) + O\left(h^4\right), j = \overline{1, n_1 - 1}. \end{cases} \quad (20)$$

The second partial derivatives w_{yy} in equation (19) are given by:

$$\begin{cases} w_{yy(i,j)} = \frac{1}{h^2}\left(-\frac{49}{18}w_{i,j} + \frac{3}{2}\left(w_{i+1,j} + w_{i-1,j}\right) - \frac{3}{20}\left(w_{i+2,j} + w_{i-2,j}\right) + \frac{1}{90}\left(w_{i+3,j} + w_{i-3,j}\right)\right) + O\left(h^6\right), i = \overline{3, n_2 - 3}, j = \overline{1, n_1 - 1}, \\ w_{yy(1,j)} = \frac{1}{h^2}\left(\frac{137}{180}w_{0,j} - \frac{49}{60}w_{1,j} - \frac{17}{12}w_{2,j} + \frac{47}{18}w_{3,j} - \frac{19}{12}w_{4,j} + \frac{31}{60}w_{5,j} - \frac{13}{180}w_{6,j}\right) + O\left(h^4\right), j = \overline{1, n_1 - 1}, \\ w_{yy(2,j)} = \frac{1}{h^2}\left(-\frac{5}{2}w_{2,j} + \frac{4}{3}\left(w_{1,j} + w_{3,j}\right) - \frac{1}{12}\left(w_{0,j} + w_{4,j}\right)\right) + O\left(h^4\right), j = \overline{1, n_1 - 1}, \\ w_{yy(n_2-1,j)} = \frac{1}{h^2}\left(\frac{137}{180}w_{n_2,j} - \frac{49}{60}w_{n_2-1,j} - \frac{17}{12}w_{n_2-2,j} + \frac{47}{18}w_{n_2-3,j} - \frac{19}{12}w_{n_2-4,j} + \frac{31}{60}w_{n_2-5,j} - \frac{13}{180}w_{n_2-6,j}\right) + O\left(h^4\right), j = \overline{1, n_1 - 1}, \\ w_{yy(n_2-2,j)} = \frac{1}{h^2}\left(-\frac{5}{2}w_{n_2-2,j} + \frac{4}{3}\left(w_{n_2-1,j} + w_{n_2-3,j}\right) - \frac{1}{12}\left(w_{n_2 j} + w_{n_2-4,j}\right)\right) + O\left(h^4\right), j = \overline{1, n_1 - 1}. \end{cases} \quad (20)$$

Similar to formulas (20), formulas for the derivative with respect to w_{xx} are written.

According to the algorithm of A. Salih [1], it is necessary first to update the values of the vortex function w at the boundary of the rectangle and only then solve the vortex equation (19) in the internal points of the cavity.

Let's expand the stream function at the first coordinate node at a distance h from the left wall along the x-axis, which is normal to the left wall:

$$\psi_1 = \psi_0 + \psi_x h + \psi_{xx}\frac{h^2}{2} + \psi_{xxx}\frac{h^3}{6} + \psi_{xxxx}\frac{h^4}{24} + \psi_{xxxxx}\frac{h^5}{120} + O\left(h^6\right). \quad (21)$$

From the equation $\overline{u} = \overline{\psi}_{\overline{y}} = 0$ it follows that on the lateral walls the stream function does not change, and from the equation $\overline{v} = -\overline{\psi}_{\overline{x}} = 0$ it follows that the stream function does not change on the bottom and top segments of the cavity. Therefore, on all four sides of the rectangular cavity, we set the stream function to be equal to zero.

Considering that on the left wall of the cavity $\psi_0 = 0, \psi_x = -v, \psi_{xx} = -w$ we rewrite equation (21) as:

$$\psi_1 = -vh - w\frac{h^2}{2} + \psi_{xxx}\frac{h^3}{6} + \psi_{xxxx}\frac{h^4}{24} + \psi_{xxxxx}\frac{h^5}{120} + O\left(h^6\right) \Leftrightarrow w = -\frac{2}{h}v - \frac{2\psi_1}{h^2} + \psi_{xxx}\frac{h}{3} + \psi_{xxxx}\frac{h^2}{12} + \psi_{xxxxx}\frac{h^3}{60} + O\left(h^4\right). \quad (22)$$

From equation (22), it can be seen that it is sufficient to approximate the derivatives of the stream function ψ_{xxx}, ψ_{xxxx},ψ_{xxxxx} at the left boundary with the 3rd, 2nd, and 1st orders of accuracy, respectively. Equation (22) has an invariant form since the order of the derivative and the step size h have the same parity. For example, for ψ_{xxxxx}, h^3 the 3rd and 5th orders, respectively, the product of the difference operator applied to ψ_{xxxxx} by h^3 does not change the sign and has the same form relative to both the right and left walls.

The program used the following approximation of derivatives for the formula (22) (in each formula (23), the index j changes within the range $j = \overline{1, n_1 - 1}$):

$$\begin{cases} w^{(3)}_{y(0,j)}h = \frac{1}{h^2}\left(-\frac{49}{8}w_{0,j} + 29w_{1,j} - \frac{461}{8}w_{2,j} + 62w_{3,j} - \frac{307}{8}w_{4,j} + 13w_{5,j} - \frac{15}{8}w_{6,j}\right) + O\left(h^4\right), \\ w^{(4)}_{y(0,j)}h^2 = \frac{1}{h^2}\left(\frac{35}{6}w_{0,j} - 31w_{1,j} + \frac{137}{2}w_{2,j} - \frac{242}{3}w_{3,j} + \frac{107}{2}w_{4,j} - 19w_{5,j} + \frac{17}{6}w_{6,j}\right) + O\left(h^4\right), \\ w^{(5)}_{y(0,j)}h^3 = \frac{1}{h^2}\left(-\frac{7}{2}w_{0,j} + 20w_{1,j} - \frac{95}{2}w_{2,j} + 60w_{3,j} - \frac{85}{2}w_{4,j} + 16w_{5,j} - \frac{5}{2}w_{6,j}\right) + O\left(h^4\right), \\ w^{(3)}_{y(n_2,j)}h = \frac{1}{h^2}\left(-\frac{49}{8}w_{n_2,j} + 29w_{n_2-1,j} - \frac{461}{8}w_{n_2-2,j} + 62w_{n_2-3,j} - \frac{307}{8}w_{n_2-4,j} + 13w_{n_2-5,j} - \frac{15}{8}w_{n_2-6,j}\right) + O\left(h^4\right), \\ w^{(4)}_{y(n_2,j)}h^2 = \frac{1}{h^2}\left(\frac{35}{6}w_{n_2,j} - 31w_{n_2-1,j} + \frac{137}{2}w_{n_2-2,j} - \frac{242}{3}w_{n_2-3,j} + \frac{107}{2}w_{n_2-4,j} - 19w_{n_2-5,j} + \frac{17}{6}w_{n_2-6,j}\right) + O\left(h^4\right), \\ w^{(5)}_{y(n_2,j)}h^3 = \frac{1}{h^2}\left(-\frac{7}{2}w_{n_2,j} + 20w_{n_2-1,j} - \frac{95}{2}w_{n_2-2,j} + 60w_{n_2-3,j} - \frac{85}{2}w_{n_2-4,j} + 16w_{n_2-5,j} - \frac{5}{2}w_{n_2-6,j}\right) + O\left(h^4\right). \end{cases} \quad (23)$$

In the work by A. Salih [1], it is pointed out that the stability of the numerical solution to problem (1) depends on the order of approximation of the boundary values of the vortex function in an equation analogous to equation (23). For example, he claims that approximating the boundary conditions of the vortex with the first order is more stable than with the second order. Using the method of splitting the vortex equation (19) with an explicit finite difference scheme, the authors did not notice any influence of the order of approximation of the vortex boundary conditions on the stability of the problem, even with a fourth-order approximation. The stability of the solution to the general problem (1) depended only on the Reynolds number Re and the choice of initial conditions.

Similarly to equation (22), for the vortex at the lower (upper) wall, we have:

$$w = \frac{2}{h}u - \frac{2\psi_1}{h^2} + \psi_{yyy}\frac{h}{3} + \psi_{yyyy}\frac{h^2}{12} + \psi_{yyyyy}\frac{h^3}{60} + O\left(h^4\right). \tag{24}$$

The profile of the initial horizontal velocity component (2), (3) and the vertical velocity component (4) refers to the deceleration method and is stable for a Reynolds number Re ≤ 3000. The acceleration method assumes initially stationary fluid in the cavity and was first proposed by A.A. Fomin and L.N. Fomina in their work [2]. The upper cover of the cavity, slowly accelerating from the stationary state, drags the fluid along with it inside the closed cavity. In work [2], the Fomins proposed the velocity of the upper cover as a function of time, according to the formula:

$$v(x,k) = 0, u(x,k) = \begin{cases} \frac{1}{2}\left(\sin\left(\frac{\pi}{2}(2t/t_1 - 1)\right) + 1\right), 0 \le t \le t_1, \\ 1, t > t_1. \end{cases}$$

In this work, the acceleration method used a similar formula:

$$v(x,k) = 0, u(x,k) = \begin{cases} \sin\left(\frac{\pi}{2}\frac{t}{t_1}\right), 0 \le t \le t_1, \\ 1, t > t_1. \end{cases} \tag{25}$$

```
horosho!                    24045 u  2.398584847328107E-003
-0.117589460964839
uu                  24045   1.26213918814584       -0.407936688073471
vv                  24045  0.241397444300957       -0.663734592934930
ww                  24045   104.601518805320        -103.604719388108
wwi0=          94 j0=          100
wwi1=         100 j1=            9
```

a)

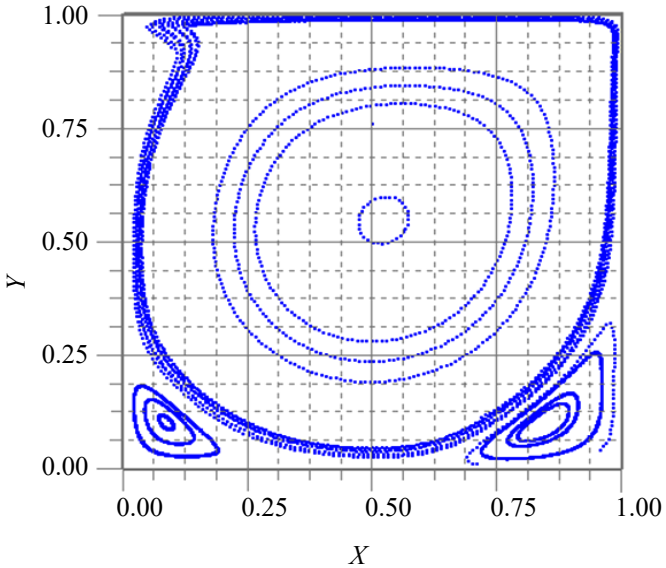

b)

Fig. 1. Results of the solution: *a* — Re = 2000, deceleration method, lower boundary of the stream function (first number), boundaries of horizontal and vertical velocity components, and vortex function at time $t = 24000$; *b* — the limiting field of streamlines in the deceleration method Re = 2000, $n_1 \times n_2 = 100 \times 100$

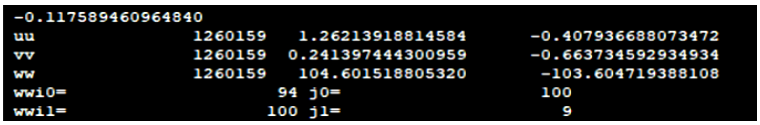

a)

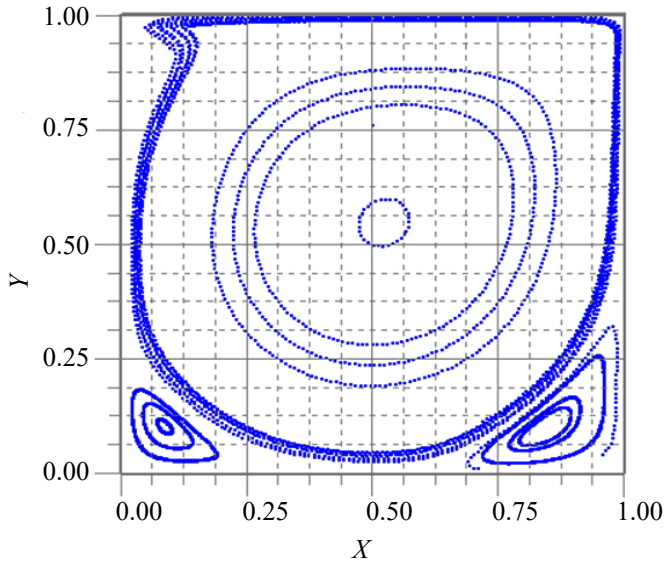

b)

Fig. 2. Results of the solution: *a* — Re = 2000, acceleration method, lower boundary of the stream function (first number), boundaries of horizontal and vertical velocity components, and vortex function at time t = 1260000; *b* — the limiting field of streamlines in the acceleration method Re = 2000, $n_1 \times n_2 = 100 \times 100$

By comparing the intervals of variation of the stream function values, the fields of horizontal and vertical velocities, and the vortex function in Figures 1 and 2, we see that they coincide with an accuracy of up to 16 significant digits. Therefore, the fields of streamlines in Figures 1 and 2 also coincide.

Thus, the acceleration and deceleration methods for the initial velocity field (2), (3), (4) are equivalent for Reynolds numbers Re ≤ 3000. However, the time required to establish steady fields in the deceleration method is tens of times (57 times) shorter than the time required to solve problem (1) using the acceleration method.

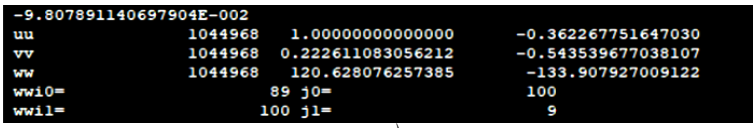

a)

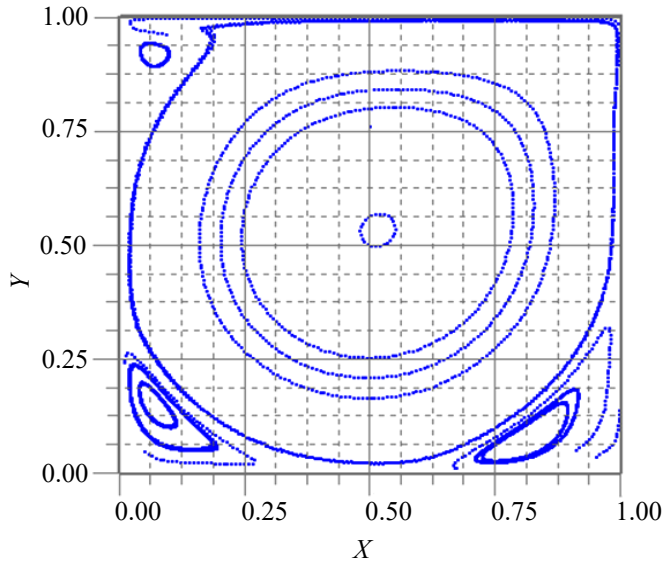

b)

Fig. 3. Results of the solution: *a* — Re = 8000, acceleration method, lower boundary of the stream function (first number), boundaries of horizontal and vertical velocity components, and vortex function at time t = 1044000; *b* — the limiting field of streamlines in the acceleration method Re = 8000, $n_1 \times n_2 = 100 \times 100$

The field of streamlines in Figure 3*b* shows three second-order vortices located at the corners of the cavity and fully coincides with the streamlines field presented in work [13, p. 22] for Re = 8000. From Figures 1, 2, and 3, it is evident that the maximum values of the vortex function occur at nodes on the upper and right walls of the cavity, near the points where the velocity profile joins or near special velocity points at the upper corners of the cavity [14].

Discussion and Conclusion. A numerical solution algorithm for a two-dimensional hydrodynamic problem in a rectangular cavity, in terms of "stream function — vortex", is proposed. The approximation of the equations in the system (1) has a sixth-order error in the interior nodes and fourth-order error in the boundary nodes. For the first time, a deceleration method with an initial horizontal velocity field is proposed using a smooth connection of two sinusoids. The initial conditions in the deceleration method are suitable for Reynolds numbers Re ≤ 3000. The numerical equivalence of solutions using the acceleration and deceleration methods is demonstrated, with final fields of the stream function, horizontal and vertical velocity components, and the vortex field coinciding up to 15 significant digits. The problem in terms of "stream function — vortex" has been numerically solved for Re = 8000 and its solution and the structure of the primary and secondary vortices qualitatively match the results of other authors.

References

1. Salih A. *Streamfunction — Vorticity Formulation*. Department of Aerospace Engineering Indian Institute of Space Science and Technology, Thiruvananthapuram; 2013:10 p.

2. Fomin A.A., Fomina L.N. The implisit iterated polynetic recurrent method in application to solving the problems of the dynamics of inconsistent fluid. *Computation research and modelling*. 2015;7(1): 35–50. (In Russ.)

3. Petrov A.G. High-precision numerical schemes for solving plane boundary value problems for a polyharmonic equation and their application to problems of hydrodynamics. *Applied Mathematics and Mechanics*. 2023;87(3):343–368 (In Russ.) https://doi.org/10.31857/S0032823523030128

4. Sukhinov A.I., Kolgunova O.V., Girmay M.Z., Nakhom O.S. A two-dimensional hydrodynamic model of coastal systems, taking into account evaporation. *Computation Mathematics and Information Technologies*. 2023;7(4):9–21. https://doi.org/10.23947/2587-8999-2023-7-4-9-21

5. Volosova N.K., Volosov K.A., Volosova A.K., Pastukhov D.F., Pastukhov Yu.F., Basarab M.A. *Collection of articles on hydrodynamics. 2nd edition*. Moscow: Moscow State Transport University of Emperor Nicholas II; 2023. 231 p. (In Russ.)

6. Ershova T.Ya. Boundary value problem for a third-order differential equation with a strong boundary layer. *Bulletin of Moscow University. Episode 15: Computational mathematics and cybernetics*. 2020;1:30–39. (In Russ.) https://doi.org/10.3103/S0278641920010057

7. Sitnikova M.A., Skulsky O.I. Flow of momentary anisotropic fluid in thin layers. *Bulletin of Perm University. Mathematics. Mechanics. Informatics*. 2015;28(1): 56–62. (In Russ.)

8. Volosov K.A., Vdovina E.K., Pugina L.V. Modeling of "pulsatile" modes of blood coagulation dynamics. *Math modeling*. 2014;26(12):14–32. (In Russ.)

9. Buzmakova M.M., Gilev V.G., Rusakov S.V. Experimental study of the rheokinetics of an epoxy binder modified with C60 fullerenes. *Bulletin of Perm University. Physics*. 2019;2:35–40. (In Russ.) https://doi.org/10.17072/1994-3598-2019-2-35-40

10. Sidoryakina V.V., Solomaha D.A. Symmetrized versions of the Seidel and upper relaxation methods for solving two-dimensional difference problems of elliptic. *Computational Mathematics and Information Technologies*. 2023;7(3):12–19. (In Russ.) https://doi.org/10.23947/2587-8999-2023-7-3-12-19

11. Volosova N.K., Volosov K.A., Volosova A.K., Karlov M.I., Pastukhov D.F., Pastukhov Yu.F. The N-fold distribution of the obvious variable scheme for the equalization of the vortex in the viscous incompatible fluid. *Bulletin of the Perm University. Mathematics. Mechanics. Informatics*. 2023;63(4):12–21. (In Russ.) https://doi.org/10.17072/1993-0550-2023-4-12-21

12. Bahvalov N.S., Zhidkov N.P., Kobelkov G.M. *Numerical methods: a textbook for students of physics and mathematics specialties of higher educational institutions.* Moscow: Binom. lab. Knowledge; 2011. 636 p. (In Russ.)

13. Kuhlmann H.C., Romano F. The Lid-Driven cavety. In book: Gelfgat A. (ed.) C*omputational Modelling of Bifurcations and Instabilities in Fluid Dynamics. Computational Methods in Applied Sciences*. Springer, Cham. 2018;50:233–309. https://doi.org/10.1007/978-3-319-91494-7_8

14. Speranskaya A.A. *Border layers in geophysical hydrodynamics:* dissertation Doctor of Physical and Mathematical Sciences. Moscow; 1982. 345 p. (In Russ.)

About the Authors:

Natalya K. Volosova, Post-graduate Student of Bauman Moscow State Technical University (2nd Baumanskaya St. 5–1, Moscow, 105005, Russian Federation), ORCID, navalosova@yandex.ru

Konstantin A. Volosov, Doctor of Physical and Mathematical Sciences, Professor of the Department of Applied Mathematics of the Russian University of Transport (Obraztsova St. 9–9, Moscow, GSP-4, 127994, Russian Federation), ORCID, SPIN-code, konstantinvolosov@yandex.ru

Aleksandra K. Volosova, Candidate of Physical and Mathematical Sciences, Chief Analytical Department "Tramplin" LLC, Russian University of Transport (Obraztsova St. 9–9, Moscow, GSP-4, 127994, Russian Federation), ORCID, SPIN-code, alya01@yandex.ru

Mikhail I. Karlov, Candidate of Physical and Mathematical Sciences, Associate Professor of the Department of Mathematics, Moscow Institute of Physics and Technology (9, Institutsky Lane, GSP-4, Dolgoprudny, 141701, Russian Federation), SPIN-code, karlov.mipt@gmail.com

Dmitriy F. Pastukhov, Candidate of Physical and Mathematical Sciences, Associate Professor of Polotsk State University (Blokhin St. 29, Novopolotsk, 211440, Republic of Belarus), ORCID, SPIN-code, dmitrij.pastuhov@mail.ru

Yuriy F. Pastukhov, Candidate of Physical and Mathematical Sciences,Associate Professor of Polotsk State University (Blokhin St. 29, Novopolotsk, 211440, Republic of Belarus), ORCID, SPIN-code, pulsar1900@mail.ru

Contributions of the authors:

N.K. Volosova: setting the task; writing a draft of the manuscript; formulation of research ideas, goals and objectives.
K.A. Volosov: scientific guidance; methodology development.
A.K. Volosova: translation; study of the history of the task; literature.
M.I. Karlov: formal analysis.
D.F. Pastukhov: visualization; validation; software.
Yu.F. Pastukhov: testing of existing code components.

Conflict of Interest Statement: **the authors declare no conflict of interest.**

All authors have read and approved the final manuscript.

Об авторах:

Наталья Константиновна Волосова, аспирант Московского государственного технического университета им. Н.Э. Баумана (105005, Российская Федерация, г. Москва, ул. 2-я Бауманская, 5, стр. 1), ORCID, navalosova@yandex.ru

Константин Александрович Волосов, доктор физико-математических наук, профессор кафедры прикладной математики Российского университета транспорта (127994, ГСП-4, Российская Федерация, г. Москва, ул. Образцова, 9, стр. 9), ORCID, SPIN-код, konstantinvolosov@yandex.ru

Александра Константиновна Волосова, кандидат физико-математических наук, начальник аналитического отдела ООО «Трамплин» Российского университета транспорта (127994, ГСП-4, Российская Федерация, г. Москва, ул. Образцова, 9, стр. 9), ORCID, SPIN-код, alya01@yandex.ru

Михаил Иванович Карлов, кандидат физико-математических наук, доцент кафедры математики Московского физико-технического института (141701, ГСП-4, Российская Федерация, г. Долгопрудный, Институтский переулок, 9), SPIN-код, karlov.mipt@gmail.com

Дмитрий Феликсович Пастухов, кандидат физико-математических наук, доцент кафедры технологий программирования Полоцкого государственного университета (211440, Республика Беларусь, г. Новополоцк, ул. Блохина, 29), ORCID, SPIN-код, dmitrij.pastuhov@mail.ru

Юрий Феликсович Пастухов, кандидат физико-математических наук, доцент кафедры технологий программирования Полоцкого государственного университета (211440, Республика Беларусь, г. Новополоцк, ул. Блохина, 29), ORCID, SPIN-код, pulsar1900@mail.ru

Заявленный вклад авторов:

Н.К. Волосова: постановка задачи; написание черновика рукописи; формулировка идей исследования, целей и задач.
К.А. Волосов: научное руководство; разработка методологии.
А.К. Волосова: перевод; изучение истории задачи; поиск литературы.
М.И. Карлов: формальный анализ.
Д.Ф. Пастухов: визуализация; валидация; разработка программного обеспечения.
Ю.Ф. Пастухов: тестирование существующих компонентов кода.

Конфликт интересов: **авторы заявляют об отсутствии конфликта интересов.**

Все авторы прочитали и одобрили окончательный вариант рукописи.

Received / Поступила в редакцию 12.02.2025
Revised / Поступила после рецензирования 19.03.2025
Accepted / Принята к публикации 28.04.2025